Nanoscale

ROYAL SOCIETY OF CHEMISTRY

COMMUNICATION

View Article Online
View Journal | View Issue

Open Access Article. Published on 17 July 2023. Downloaded on 11/9/2025 10:14:23 PM.
This article is licensed under a Creative Commons Attribution 3.0 Unported Licence.

Check for updates

Cite this: *Nanoscale*, 2023, **15**, 12476

Received 9th May 2023,
Accepted 14th July 2023

DOI: 10.1039/d3nr02160b

rsc.li/nanoscale

Fluorescent imaging using novel conjugated polymeric nanoparticles-affimer probes in complex *in vitro* models of colorectal cancer†

Precious Jolugbo, ‡[a] Thomas Willott,‡[a] Wei-Hsiang Lin,[b] Thomas Maisey,[a] Dermott O'Callaghan,[c] Mark A. Green,[c,d] David G. Jayne[a] and M. Ibrahim Khot *[a]

We developed a carcinoembryonic antigen (CEA) conjugated polymer nanoparticle (CPN510-CEA-Af) probe to target CEA-expressing CRC cells *in vitro*. Its efficacy was evaluated in 2D and 3D cultures of LS174T, LoVo, and HT29 CRC cell lines. CPN510-CEA-Af produced greater fluorescent signal intensity than unconjugated particles in both 2D cells and 3D spheriods, indicating its potential as a probe for image-guided colorectal cancer surgery.

Colorectal cancer (CRC) is the third most common cancer, and fourth leading cause of cancer-related mortality worldwide, accounting for over 900 000 deaths annually.[1] Complete surgical resection is the mainstay of curative treatment for CRC.[2] However, despite a complete excision of the tumour, over 24% of patients who undergo curative surgery either develop local recurrence or metastases.[3]

There has been an increasing interest in using fluorescence-guided surgery for CRC to delineate between cancerous and healthy tissues. Systematically administered fluorophores have been used during surgery to facilitate tumour localisation and aid complete oncological resection, whilst reducing unnecessary damage to the surrounding healthy tissue.[4,5] To improve the biological applications of these fluorescent probes, newly developed fluorescent fluorophores have been created using a diverse range of materials such as quantum dots, carbon dots and nanoparticles.[6] In particular, conjugated polymeric nanoparticles (CPNs) have demonstrated significant potential in drug delivery, improved biocompatibility and the ability to be easily functionalised.[6] CPNs have many advantages over traditional dyes, such as intense photoluminescence in both the visible range of light and NIR spectrum and have been widely validated across a range of biological applications, specifically in fluorescence-based applications, such as lateral flow assays,[7] flow cytometry,[8] and photothermal therapy. In addition, they have recently been evaluated in imaging CRC cells for tumour delineation, however targeting molecules were not used.[9] Although several fluorescent probes have been examined for their potential use in surgical procedures, only four have been approved for clinical use to date.[5] This limited selection is frequently attributed to the rapid clearance from living systems, poor photostability, non-specific protein binding, and non-specific targeting exhibited by many probes. Consequently, there is a pressing need to develop a new generation of fluorophores that exhibit high sensitivity and specificity in distinguishing cancerous tissue from healthy tissue, while also maintaining its fluorescent intensity and minimal toxicity.

The conjugation of a fluorophore with a targeting ligand that selectively identifies over-expressed biomarkers in CRC has been already been proposed.[10] Various biomarkers are often overexpressed in CRC cells, including carcinoembryonic antigen (CEA), tumour-associated glycoprotein 72 (TAG-72), endothelial growth factor receptor (EGFR), and folate receptor alpha (FRα).[11] CEA has been shown to be overexpressed in 98.8% of CRC tumours[12] making it an attractive target for tumour localisation. Ligands such as aptamers, peptides and antibodies are often used as moieties for the targeted delivery of diagnostic and therapeutic agents.[13] Antibodies are commonly used ligands that bind to specific antigens with high target specificity and sensitivity and have a long serum half-life.[14,15] However, recent studies have highlighted the difficulties of using antibody ligands, such as immunogenicity, rapid clearance, poor stability, and lower than predicted effectiveness due to batch-to-batch variability.[16–20] To overcome the antibody-based limitations, alternative targeting ligands have been explored.[21–25] Affimers are small and stable recombinant proteins offering many advantages to conventional monoclonal antibodies.[26] Affimers are produced as a single domain with no disulphide bridges or post-translational modifications, allowing for structural simplicity.[27] They consist of small

[a]*Leeds Institute of Medical Research at St James', School of Medicine, St James University Hospital, University of Leeds, Leeds, LS9 7TF, UK.*
E-mail: M.I.Khot@leeds.ac.uk
[b]*Faculty of Biology, Medicine and Health, The University of Manchester, Manchester, M13 9PL, UK*
[c]*Stream Bio Ltd, Alderley Park, Nether Alderley, Cheshire, SK10 4TG, UK*
[d]*Department of Physics, Faculty of Natural, Mathematical & Engineering Sciences, King's College London, Strand, London, WC2R 2LS, UK*

† Electronic supplementary information (ESI) available. See DOI: **https://doi.org/10.1039/d3nr02160b**

‡ These authors equally contributing.

This journal is © The Royal Society of Chemistry 2023

Open Access Article. Published on 17 July 2023. Downloaded on 11/9/2025 10:14:23 PM.
This article is licensed under a Creative Commons Attribution 3.0 Unported Licence.

synthetic protein scaffolds (12–14 kDa) based on cystatins or human steffin A, which is about one-tenth the size of a typical antibody.[25,28] They can be conjugated to fluorophores in a more controlled and site-specific manner, improving target binding and increased sensitivity.[25]

In this study, we assessed the *in vitro* efficacy and cytotoxicity of anti-CEA conjugated polymeric nanoparticles (CPN510-CEA-Af) as fluorescent probes using 2D monoculture and 3D multicellular spheroid CRC models.

Results and discussion

In order to assess the effectiveness of CPN510-CEA Af in identifying and selectively binding to CRC cells expressing CEA, immunofluorescence staining was performed on a subset of cell lines (LS174T, LoVo, HT29, and EA.hy926) to evaluate the extent of CEA expression. The cells were incubated with a primary anti-CEA antibody, followed by a secondary antibody conjugated with Alexa Fluor 488, and subsequently stained with DAPI. Immunofluorescence demonstrated different levels of fluorescence intensity in the various CRC cell lines, indicating different expression of the CEA antigen (Fig. 1). LS174T and LoVo showed the highest CEA expression, with HT29 showing moderate/low expression. This has been confirmed in previous studies investigating the expression of CEA in CRC cells.[29] No CEA protein expression was observed in EA.hy926 cells, suggesting that this cell line is appropriate to use as a control for the anti-CEA Affimer.

Traditionally, fluorescent probes with maximal absorption in the near-infrared range (NIR) offer various advantages over shorter wavelength visible light, including greater tissue penetration of light, reducing adverse haemoglobin and water absorption and reduced autofluorescence from adjacent tissues.[30] Conjugated polymer nanoparticle were chosen for this study as they have been developed to overcome the inherent disadvantages of non-NIR fluorescent probes, due to their intense brightness, physical and chemical stability and negligible photobleaching, making them highly sensitive.[31]

The cytotoxicity of a commercially available conjugated polymer nanoparticle system, emitting at 510 nm (CPN510), was explored at different concentrations (0.1 mg ml^{-1}, 0.05 mg ml^{-1}, 0.02 mg ml^{-1}) by incubation of the particles with a range of cells, after which cell viability was measured. As shown in Fig. 2, no significant reduction in cell viability was observed in all cell lines and all concentrations of CPN510. Cell viability remained at >90%. No significant difference was found between control and treated cell cultures ($p > 0.05$ at all concentrations). This confirmed CPN510 to be minimally cytotoxic and biocompatible. The biocompatibility of CPN510 allowed the nanoparticle to be used for the diagnosis and imaging of CRC tissue, without inducing adverse cytotoxicity.

Although the CPNs are mainly organic in composition, the materials are also magnetic due to the presence of iron oxide in the particles which also needs to be considered. The lack of toxicity is in line with several studies that investigated the cytotoxicity of iron oxide-containing nanoparticles. Marcus *et al.* investigated the cytotoxicity of uncoated maghemite iron oxide nanoparticles in rat pheochromocytoma PC12 cells and found cell viability to exceed 90% at 0.1 mg ml^{-1} but reduced to 51% at 0.25 mg ml^{-1} iron oxide nanoparticles.[32] Several iron oxide-based nanoparticles have been approved by the FDA for diagnostic use.[33,34] Another study by Naqvi *et al.* found 95% cell viability in murine macrophage cells (J774) incubated with superparamagnetic iron oxide nanoparticles, decreasing to 55–66% cell viability after prolonged exposure.[35]

Unconjugated and CEA Affimer conjugated CPN510 were incubated with 2D CRC monolayers and 3D multicellular CRC

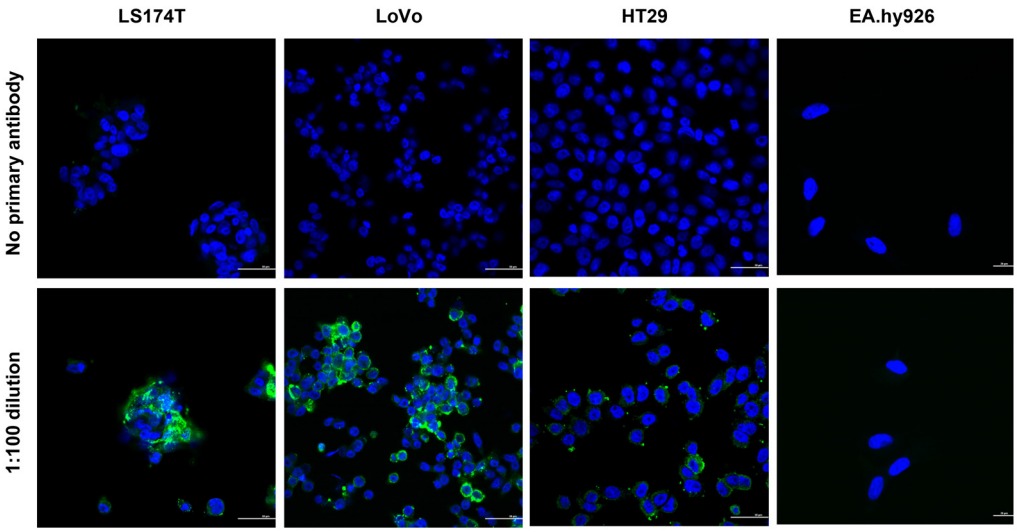

Fig. 1 Immunofluorescence staining of LS174T, LoVo, HT29 and EA.hy926. Cells were incubated with primary anti-CEA antibody followed by Alexa Fluor 488-conjugated secondary antibody (green fluorescence). Cells were also stained with DAPI (blue fluorescence). Scale bar = 50 μm; except EA.hy926 = 20 μm. Images are representative of 3 independent experiments.

Open Access Article. Published on 17 July 2023. Downloaded on 11/9/2025 10:14:23 PM.
This article is licensed under a Creative Commons Attribution 3.0 Unported Licence.

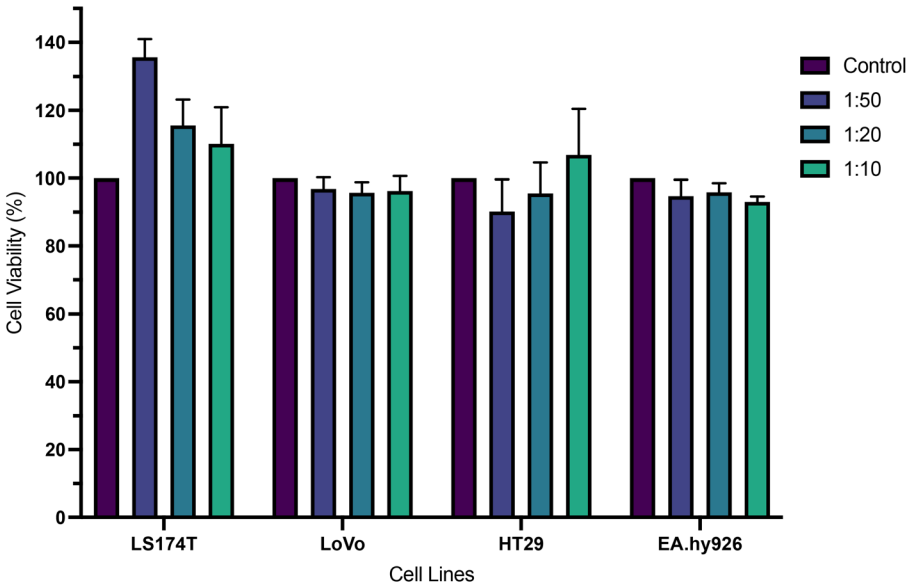

Fig. 2 Cell viability of LS174T, LoVo, HT29 and EA.hy926 cells treated with CPN510 nanoparticles. Cells were treated with different concentrations of the CPN510 nanoparticle for 24 hours and cell viability was quantified using MTT assay. $N = 4$. Data are presented as mean values ± SEM.

spheroids. As demonstrated in Fig. 3, CEA Affimer conjugation improved the uptake of CPN510 into CEA-positive CRC cells (LS174T, LoVo and HT29) as compared to unconjugated CPN510. No difference in fluorescence was found between CPN510-CEA-Af and unconjugated CPN510 treated EA.hy926 cells. These findings were replicated in 3D multicellular CRC spheroids of LS174T and HT29 cells with increased fluorescence observed in CPN510-CEA-Af indicating increased CEA Affimer mediated CPN510 uptake (Fig. 4A).

A 4-fold ($p < 0.0148$), 5-fold ($p < 0.0002$) and 9-fold ($p < 0.0001$) increase in fluorescence intensity was observed in 2D LS174T, LoVo and HT29 cells respectively, treated with CPN510-CEA-Af, as compared to unconjugated CPN510 (Fig. 4B). No difference in fluorescence intensity was detected in EA.hy926 cells incubated with CPN510-CEA-Af as compared to unconjugated CPN510. A 3-fold increase in fluorescence intensity was observed in 3D spheroidal models of both LS174T and HT29 cells treated with CPN510-CEA-Af as com-

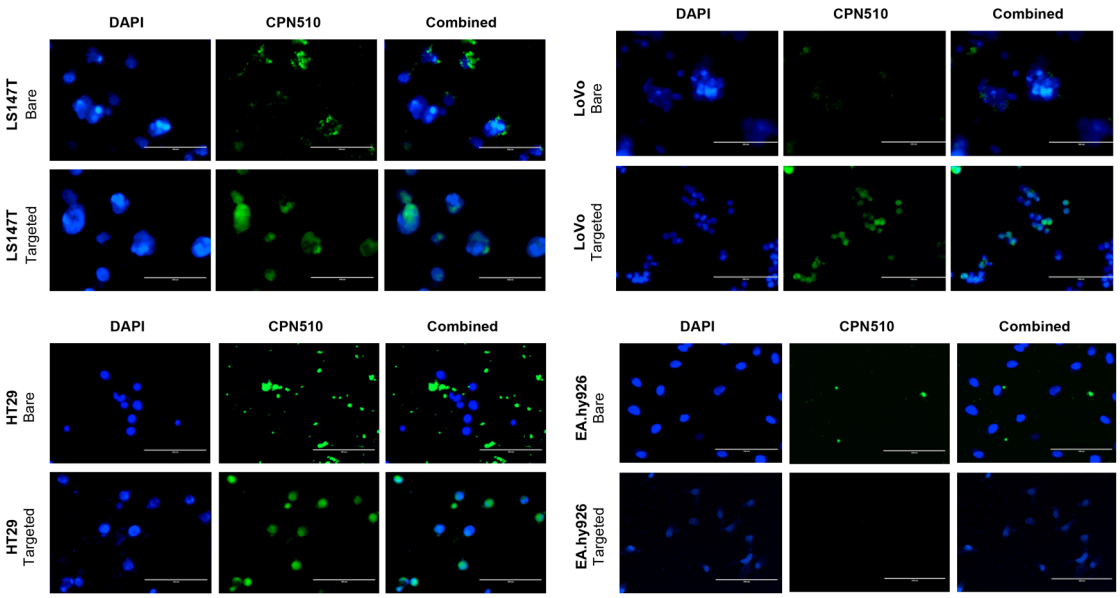

Fig. 3 2D monolayer LS174T, LoVo, HT29 and EA.hy926 cells were cultured on cover slips and incubated with CEA Affimer conjugated and unconjugated CPN510 nanoparticles (green fluorescence). Cells were also co-treated with Hoechst 33342 (blue fluorescence). Scalebar = 100 μm.

 This journal is © The Royal Society of Chemistry 2023

Open Access Article. Published on 17 July 2023. Downloaded on 11/9/2025 10:14:23 PM.
This article is licensed under a Creative Commons Attribution 3.0 Unported Licence.

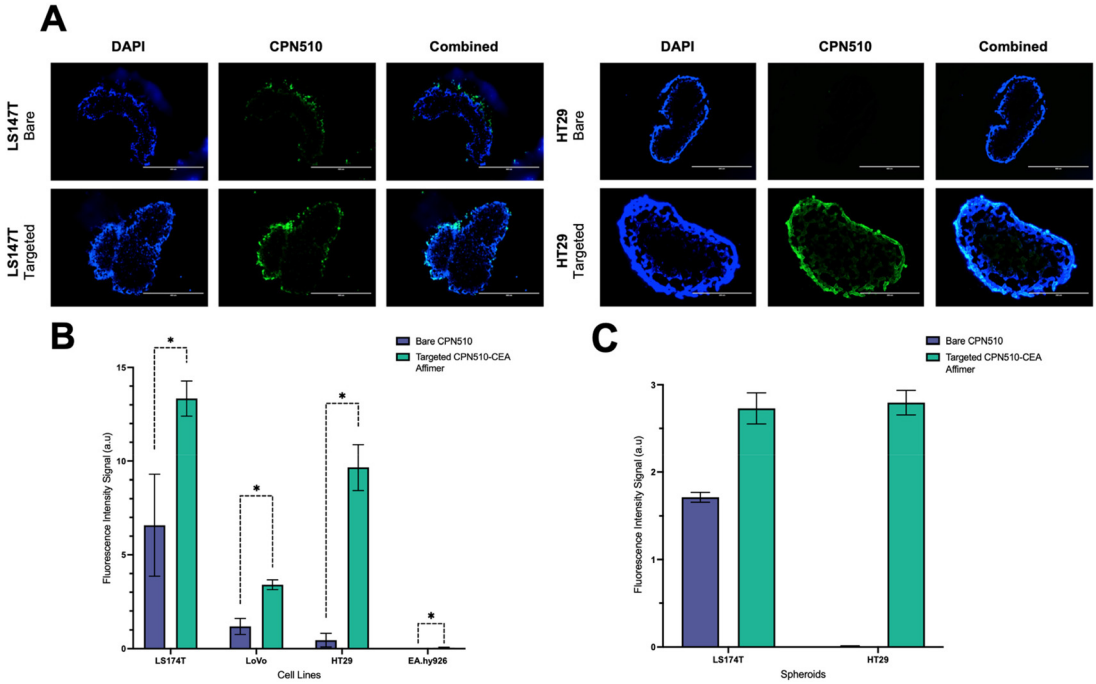

Fig. 4 (A). 3D spheroidal models of LS174T and HT29 cells were grown in Ultra Low Attachment multiwell plates and incubated with CEA Affimer conjugated and unconjugated CPN510 nanoparticles (green fluorescence). Cells were also co-treated with Hoechst 33342 (blue fluorescence). Scalebar = 400 μm. Images are representative of 2 independent experiments. (B) 2D cell cultures of LS174T, LoVo, HT29 and EA.hy926 cells were treated CPN510-CEA-Af and unconjugated CPN510. ImageJ was used to quantify fluorescence intensity. *$p < 0.05$. (C) Graph showing the fluorescence intensity signal of both unconjugated CPN510 and CPN510-CEA-Af in 3D multicellular spheroids. ImageJ was used to quantify the fluorescence intensity.

pared to unconjugated CPN510 (Fig. 4C). These findings are consistent with prior investigations that have attempted to conjugate a targeting ligand to a fluorophore for the purpose of cancer imaging. Specifically, Tiernan *et al.* reported that cells targeted with CEA exhibited a significantly greater fluorescence signal intensity relative to control cells ($p < 0.002$).[36] Similarly, Kogan-Zviagin *et al.* demonstrated that a targeted fluorescent probe attached strongly to cancerous tissue in CRC cells, while displaying minimal accumulation in healthy tissue specimens.[37] Furthermore, they observed a positive correlation between the intensity of fluorescence in cells treated with the fluorophore and the level of antigen expression. Despite substantial evidence supporting the utilization of fluorescent probes to enhance tumour identification, Shamsuddin *et al.* noted that Affimers produced more intense staining than immunostaining, which requires the use of antibodies.[26] This was attributed to their smaller size, which allows for greater penetration into fixed cells. Notably, our study presents a novel approach involving the development of a fluorescent probe conjugated with anti-CEA Affirmers for potential use in fluorescence-guided surgery.

Conclusions

This study demonstrates the efficacy of the Affimer-conjugated polymer nanoparticle in targeting 2D and 3D *in vitro* models of CRC expressing the CEA antigen. CPN510-CEA-Af has the potential to be a useful tool for fluorescent-guided surgery CRC. Further characterisation of CPN510-CEA-Af is required using *in vivo* models of CRC to progress it towards clinical application.

Author contributions

D. O'C., A. C., M. A. G., D. G. J. and M. I. K. conceptualised the overall study. P. J., T. W. and W.-H. L., conducted the experiments and data analysis. T. M., D. O'C. and M. I. K. developed experimental protocols. P. J., M. A. G., D. G. J. and M. I. K. wrote and edited the manuscript. All authors approve the final manuscript.

Conflicts of interest

There are no conflicts to declare.

Acknowledgements

MG acknowledges funding *via* EPSRC (EP/X014495/1). DGJ acknowledges funding from Bowel Cancer UK and the UK National Institute of Health Research (Bowel Cancer UK: 18SC0001NIHR: NIHR203744).

Open Access Article. Published on 17 July 2023. Downloaded on 11/9/2025 10:14:23 PM.
This article is licensed under a Creative Commons Attribution 3.0 Unported Licence.

References

1 E. Dekker, P. J. Tanis, J. L. A. Vleugels, P. M. Kasi and M. B. Wallace, *Lancet*, 2019, **394**, 1467–1480.
2 T. Matsuda, K. Yamashita, H. Hasegawa, T. Oshikiri, M. Hosono, N. Higashino, M. Yamamoto, Y. Matsuda, S. Kanaji, T. Nakamura, S. Suzuki, Y. Sumi and Y. Kakeji, *Ann. Gastroenterol. Surg.*, 2018, **2**, 129–136.
3 D. Luo, Y. Yang, Z. Shan, Q. Liu, S. Cai, Q. Li and X. Li, *Front. Surg.*, 2021, **8**, 666400.
4 S. Keereweer, P. B. Van Driel, T. J. Snoeks, J. D. Kerrebijn, R. J. Baatenburg de Jong, A. L. Vahrmeijer, H. J. Sterenborg and C. W. Löwik, *Clin. Cancer Res.*, 2013, **19**, 3745–3754.
5 T. Nagaya, Y. A. Nakamura, P. L. Choyke and H. Kobayashi, *Front. Oncol.*, 2017, **7**, 314.
6 Y. Du, N. Alifu, Z. Wu, R. Chen, X. Wang, G. Ji, Q. Li, J. Qian, B. Xu and D. Song, *Front. Bioeng. Biotechnol.*, 2020, **8**, 1029.
7 StreamBio, CPN™ vs europium chelate comparison, **https://www.streambio.co.uk/cpn-vs-europium-chelate-comparison/**, (accessed 15 June 2022, 2022).
8 StreamBio, Flow Cytometry & Spectral Flow Cytometry, **https://www.streambio.co.uk/our-technology/cpn-case-studies/flow-cytometry/**, (accessed 15 June 2022, 2022).
9 StreamBio, Colon Cancer Cell Imaging, **https://www.streambio.co.uk/our-technology/cpn-case-studies/colon-cancer-cell-imaging/**, (accessed 15 June 2022, 2022).
10 P. Debie and S. Hernot, *Front. Pharmacol.*, 2019, **10**, 510.
11 B. A. Alves Martins, G. F. de Bulhões, I. N. Cavalcanti, M. M. Martins, P. G. de Oliveira and A. M. A. Martins, *Front. Oncol.*, 2019, **9**, 1284.
12 J. P. Tiernan, S. L. Perry, E. T. Verghese, N. P. West, S. Yeluri, D. G. Jayne and T. A. Hughes, *Br. J. Cancer*, 2013, **108**, 662–667.
13 Z. Zhao, A. Ukidve, J. Kim and S. Mitragotri, *Cell*, 2020, **181**, 151–167.
14 A. M. Scott, J. D. Wolchok and L. J. Old, *Nat. Rev. Cancer*, 2012, **12**, 278–287.
15 S. Sharma, H. Byrne and R. J. O'Kennedy, *Essays Biochem.*, 2016, **60**, 9–18.
16 D. A. Richards, A. Maruani and V. Chudasama, *Chem. Sci.*, 2017, **8**, 63–77.
17 V. H. Shargh, H. Hondermarck and M. Liang, *Nanomedicine*, 2016, **11**, 63–79.
18 Y. Wang, A. M. Dossey, J. W. Froude 2nd, S. Lubitz, D. Tzur, V. Semenchenko and D. S. Wishart, *Nanomedicine*, 2008, **3**, 475–483.
19 R. E. Kontermann, *Curr. Opin. Mol. Ther.*, 2006, **8**, 39.
20 S. D. Steichen, M. Caldorera-Moore and N. A. Peppas, *Eur. J. Pharm. Sci.*, 2013, **48**, 416–427.
21 J. Löfblom, J. Feldwisch, V. Tolmachev, J. Carlsson, S. Ståhl and F. Y. Frejd, *FEBS Lett.*, 2010, **584**, 2670–2680.
22 A. Koide, C. W. Bailey, X. Huang and S. Koide, *J. Mol. Biol.*, 1998, **284**, 1141–1151.
23 A. Plückthun, *Annu. Rev. Pharmacol. Toxicol.*, 2015, **55**, 489–511.
24 A. Skerra, *FEBS J.*, 2008, **275**, 2677–2683.
25 C. Tiede, R. Bedford, S. J. Heseltine, G. Smith, I. Wijetunga, R. Ross, D. Alqallaf, A. P. Roberts, A. Balls, A. Curd, R. E. Hughes, H. Martin, S. R. Needham, L. C. Zanetti-Domingues, Y. Sadigh, T. P. Peacock, A. A. Tang, N. Gibson, H. Kyle, G. W. Platt, N. Ingram, T. Taylor, L. P. Coletta, I. Manfield, M. Knowles, S. Bell, F. Esteves, A. Maqbool, R. K. Prasad, M. Drinkhill, R. S. Bon, V. Patel, S. A. Goodchild, M. Martin-Fernandez, R. J. Owens, J. E. Nettleship, M. E. Webb, M. Harrison, J. D. Lippiat, S. Ponnambalam, M. Peckham, A. Smith, P. K. Ferrigno, M. Johnson, M. J. Mcpherson and D. C. Tomlinson, *eLife*, 2017, **6**, e24903.
26 S. H. Shamsuddin, D. G. Jayne, D. C. Tomlinson, M. J. Mcpherson and P. A. Millner, *Sci. Rep.*, 2021, **11**, 744.
27 M. Johnson, *Bioanalysis*, 2020, **12**, 125–128.
28 L. K. J. Stadler, T. Hoffmann, D. C. Tomlinson, Q. Song, T. Lee, M. Busby, Y. Nyathi, E. Gendra, C. Tiede, K. Flanagan, S. J. Cockell, A. Wipat, C. Harwood, S. D. Wagner, M. A. Knowles, J. J. Davis, N. Keegan and P. Ko Ferrigno, *Protein Eng., Des. Sel.*, 2011, **24**, 751–763.
29 F. M. K. Elekonawo, D. L. Bos, D. M. Goldenberg, O. C. Boerman and M. Rijpkema, *EJNMMI Res.*, 2019, **9**, 108.
30 N. Kosaka, M. Ogawa, P. L. Choyke and H. Kobayashi, *Future Oncol.*, 2009, **5**, 1501–1511.
31 StreamBio., Our Technology, **https://www.streambio.co.uk/our-technology/**, (accessed 16 June 2022, 2022).
32 M. Marcus, M. Karni, K. Baranes, I. Levy, N. Alon, S. Margel and O. Shefi, *J. Nanobiotechnol.*, 2016, **14**, 37.
33 J. Gallo, N. J. Long and E. O. Aboagye, *Chem. Soc. Rev.*, 2013, **42**, 7816–7833.
34 O. Veiseh, J. W. Gunn and M. Zhang, *Adv. Drug Delivery Rev.*, 2010, **62**, 284–304.
35 S. Naqvi, M. Samim, M. Abdin, F. J. Ahmed, A. Maitra, C. Prashant and A. K. Dinda, *Int. J. Nanomed.*, 2010, **5**, 983–989.
36 J. P. Tiernan, N. Ingram, G. Marston, S. L. Perry, J. V. Rushworth, P. L. Coletta, P. A. Millner, D. G. Jayne and T. A. Hughes, *Nanomedicine*, 2015, **10**, 1223–1231.
37 I. Kogan-Zviagin, Y. Shamay, A. Nissan, O. Sella-Tavor, M. Golan and A. David, *J. Controlled Release*, 2014, **192**, 182–191.

This journal is © The Royal Society of Chemistry 2023